The Immune Deficiency Pathway Attenuates Insulin Signaling to Protect Against Infection.

Saeideh Davoodi[1], Meghan Ferguson[1], Rujuta Despahnde[2], Savraj Grewal[2], Edan Foley[1]*.

1. Department of Medical Microbiology and Immunology

   Faculty of Medicine and Dentistry

   University of Alberta

   Edmonton

   Alberta T6G 2S2, Canada.

2. Clark H Smith Brain Tumour Centre

   Arnie Charbonneau Cancer Institute

   Alberta Children's Hospital Research Institute

   and Department of Biochemistry and Molecular Biology Calgary

   University of Calgary

   Alberta T2N 4N1, Canada

*Corresponding author.

Email: efoley@ualberta.ca

ABSTRACT

Immune and metabolic pathways collectively contribute to the containment of microbial invaders, and persistent activation of immune responses contribute to the development of severe metabolic disorders. To determine how a prolonged immune response impacts metabolism, we induced a constitutive inflammatory response in the *Drosophila* fat body, a key regulator of humoral immunity and metabolic homeostasis. We found that persistent immune activity replicated key features of a suppressed insulin pathway - delayed development, depleted fat reserves, and hyperglycemia. These observations led us to ask if the inhibition of insulin signaling improves host survival after infection. To test this, we challenged insulin pathway mutants with lethal doses of the enteric pathogen, *Vibrio cholerae*. We found that loss-of-function mutations in the insulin pathway extended viability and lowered bacterial loads, while gain-of-function mutations diminished viability and elevated bacterial loads. Combined, our results support a role for immune regulation of the insulin pathway in the survival of microbial challenges.

INTRODUCTION

Barrier tissues shield an animal from an immeasurable number of molecular hazards in their immediate environment. For example, the gastrointestinal tract processes a complex mixture of ingested material in a manner that blocks microbial penetration of the host interior, while allowing an orderly flow of essential nutrients to metabolic organs. Once inside the host, nutrients initiate the transduction of signals through metabolic pathways that control organ growth and development. Prominent metabolic regulators appeared very early during animal evolution - an estimated billion years ago in the case of the insulin peptides (Le Roith *et al.*, 1980), and execute conserved functions across the animal kingdom. Insulin peptides control the uptake and storage of nutrients, activate cellular growth, and influence longevity in worms, flies, and rodents (Gems and Partridge, 2013; Kannan and Fridell, 2013; Murphy and Hu, 2013).

Metabolism undergoes a fundamental shift during times of microbial infection (O'Neill, Kishton and Rathmell, 2016). At this point, germline-encoded pattern recognition receptors detect the molecular signatures of alien microbes, and initiate physiological responses designed to neutralize the invader, and optimize host survival. We frequently focus on immunity as the generation of potent bactericidal molecules that rapidly eliminate the invader. However, microbial detection initiates a complex spectrum of physiological responses, that may include elements as diverse as increased body temperature, lethargy, loss of appetite, social isolation, and tolerance mechanisms that neutralize pathogens without affecting their numbers (Ayres and Schneider, 2012). Metabolic adaptations are common to host responses to infection (Eisenreich *et al.*, 2013). In this case, hosts balance their traditional metabolic needs against the immediate threat presented by the microbe, and frequently alter metabolic pathway activity accordingly.

The integration of immune and metabolic pathways is particularly apparent in insects such as *Drosophila melanogaster* where the fat body simultaneously regulates energy storage and humoral immunity. Under optimal conditions, the larval fat body detects circulating sugars and amino acids in the hemolymph to control the release of *Drosophila* Insulin-Like Peptides (dILPs) from the brain (Boulan, Milán and Léopold, 2015). dILPs enter circulation and orchestrate the activity of metabolic organs such as muscle, and fat. At the same time, pattern recognition receptors survey the hemolymph for microbe-associated molecular patterns that indicate microbial invasion. Several classes of microbe activate Toll-mediated responses in the fat body (Valanne, Wang and Ramet, 2011), while the Immune Deficiency (IMD) pathway, an evolutionary relative of the TNF pathway (Myllymaki, Valanne and Ramet, 2014), responds to diaminopimelic peptidoglycan (Buchon, Silverman and Cherry, 2014). The host integrates cues from these immune and metabolic pathways to determine the net output of the fat body. For example, under times of high nutrient availability, and limited microbial detection, the *Drosophila* MEF2 transcription factor is phosphorylated, and promotes lipogenesis and glycogenesis, molecular pathways that support long-term growth in the animal (Clark *et al.*, 2013). However, sudden activation of immune responses causes a loss of MEF2 phosphorylation, an event that shifts fat body activity from the accumulation of energy stores to the release of antimicrobial peptides. Such metabolic shifts, are common in *Drosophila* responses to infection, and frequently include alterations to the activity of insulin pathway elements (Dionne *et al.*, 2006; Chambers, Song and Schneider, 2012).

Molecular links between immune and metabolic pathways are conserved across vast evolutionary distances, and are essential for homeostasis and long-term survival. For example, inflammation is involved in the development of chronic metabolic disorders such as insulin resistance, and type two diabetes (Wellen and Hotamisligil, 2005; Lee, 2013). In experimental models of obesity, adipose tissue-resident macrophages produce TNF (Weisberg *et al.*, 2003; Xu *et al.*, 2003), and TNF contributes to the

development of obesity-induced insulin resistance (Hotamisligil, Shargill and Spiegelman, 1993a; Uysal *et al.*, 1997; Uysal, Wiesbrock and Hotamisligil, 1998). Indeed, treatment with anti-inflammatory salicylates improves obesity-induced insulin resistance, and type two diabetes (Kim *et al.*, 2001; Yuan *et al.*, 2001). However, despite the impact of inflammatory cues on metabolic homeostasis, we do not fully understand how the respective pathways communicate.

To address this question, we used the *Drosophila* model to determine the physiological impacts of persistent IMD activity on host metabolism. As expected, activation of IMD leads to a robust antibacterial response. However, our work also showed that chronic IMD activity has the molecular, genetic, and phenotypic signatures of a depressed insulin pathway. Transcriptionally, activation of IMD resulted in a gene expression signature consistent with diminished insulin pathway activity. Physiologically, IMD caused a depletion of lipid stores, hyperglycemia, delayed development, and a reduction in adult size. The conservation of IMD/TNF-dependent regulation of insulin signaling between flies and mammals led us to speculate that suppression of insulin has survival benefits during infection. To test this hypothesis, we characterized immune responses in flies with insulin pathway mutations. We found that hypomorphic mutations in the insulin pathway enhanced host survival, and diminished pathogen load, while hypermorphic mutations diminished host survival, and increased pathogen load. Combined these results lead us to propose that the IMD/TNF axis regulates insulin pathway activity as part of an adaptive response to microbial infection.

RESULTS

Activation of IMD in the fat body modifies metabolism.

The fat body coordinates nutrient utilization with humoral immunity to support the growth and viability of *Drosophila*. At present, we do not know the extent to which metabolic shifts are directly controlled by host immunity. Most microbial challenges to *Drosophila* involve feeding flies a palatable diet soiled with pathogenic bacteria, or puncturing the exoskeleton with a contaminated needle. Both procedures induce antimicrobial responses, but invariably involve parallel adaptations to microbial, or mechanical, destruction of host tissue. To directly examine the effects of IMD pathway activation on host physiology, we used the R4GAL4 driver line to express a constitutively active IMD (ImdCA) construct exclusively in the fat body (*R4/imdCA*).

Initially, we used whole-genome microarray analysis to compare the global transcription profiles of *R4/imdCA* larvae to control, age-matched *R4GAL4/+* (*R4/+*) larvae. Activation of IMD in larval fat deregulated the expression of 1188 genes in third instar larvae (Tables 1 and 2). We confirmed deregulated expression for six representative genes in subsequent qPCR assays (Figure 1). As expected, many of the response genes, such as antimicrobial peptides, have established roles in the elimination of microbial invaders (Figure 2A-C). However, we also noted substantial effects of IMD activation on the expression of genes that control metabolism (Figure 2A-C, Tables 1 and 2). Of the 807 IMD response genes with annotated biological functions, 247 are classified as regulators of metabolic processes (Figure 2C). For example, activation of IMD caused a downregulation of TOR pathway genes (Figure 2B); decreased the expression of *dilp3* (Figure 2D); increased the expression of the insulin pathway antagonists *dilp6*, and *impl2* (Figure 2D); and elevated expression of the FOXO-responsive transcripts *thor*, and *tobi* (Figure 2D). Consistent with effects of IMD activation on host metabolism, we observed a significant reduction in the expression of enzymes involved in glycolysis, the TCA cycle, mitochondrial

ATP production, and fatty acid beta oxidation (Figure 2A, Figure 3, Table 1). We also noted that host responses to IMD activation extend beyond the fat body, as IMD activation suppressed the expression of intestinal peptidases and chitin-binding proteins, and lowered the expression of hormone signaling molecules in the salivary glands (Table 1).

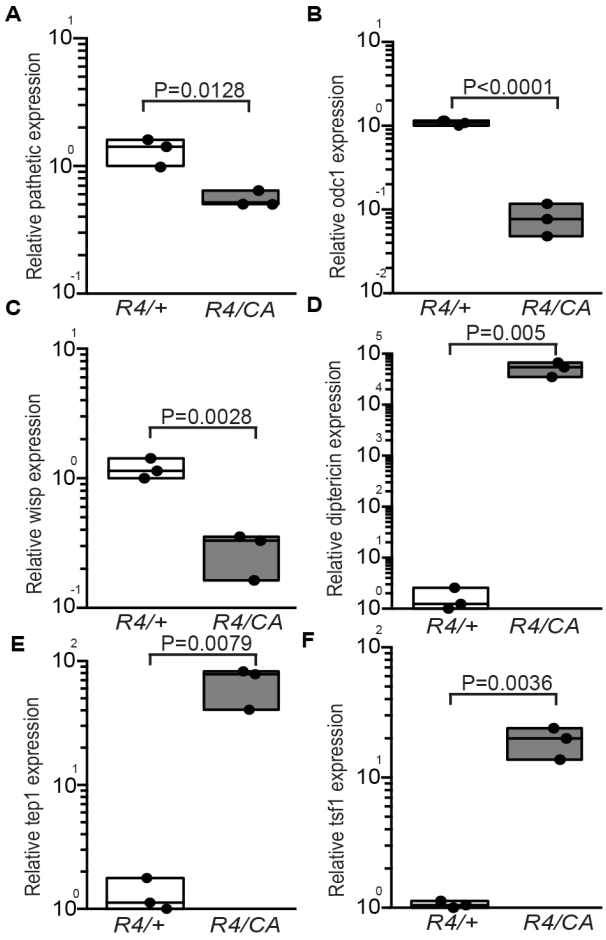

Figure 1. Quantification of gene expression in *R4/+* and *R4/ImdCA* larvae. Relative gene expression from third instar *R4/ImdCA* and *R4/+* larvae. All statistical significance was determined using a Student's t test.

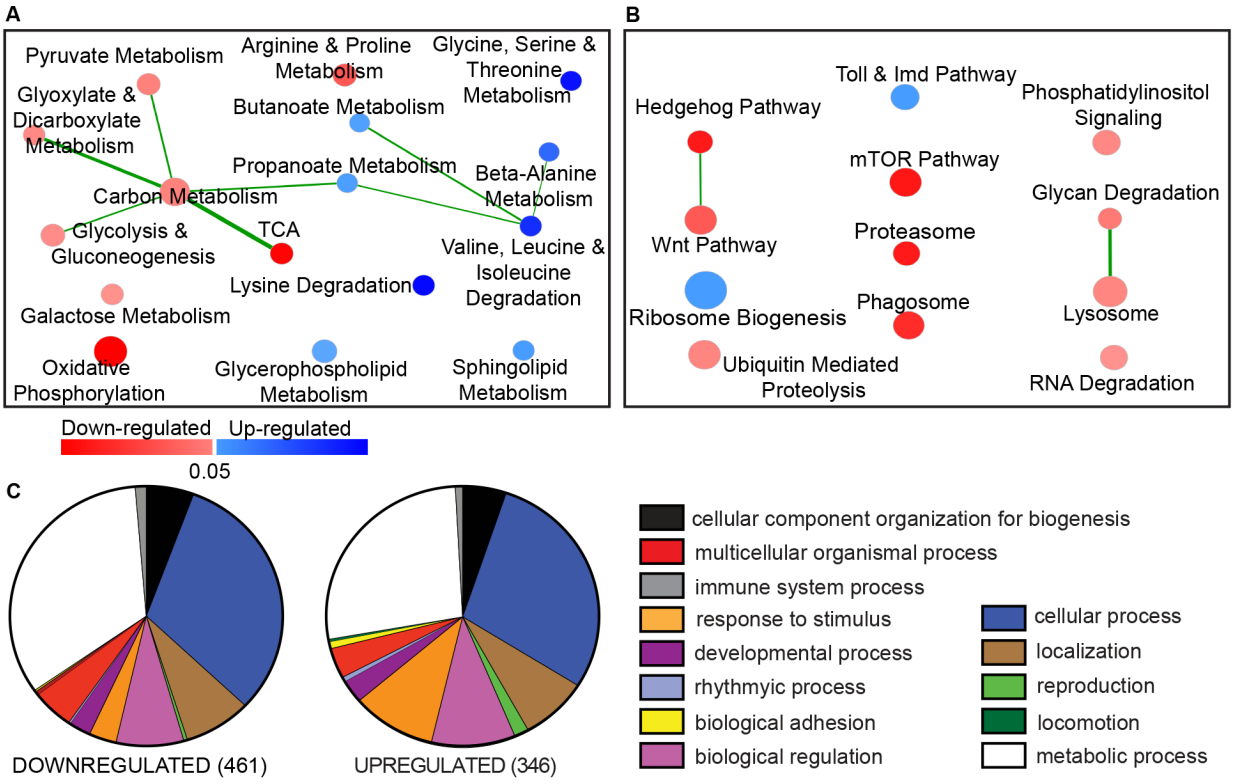

D

Gene	Function	Fold change R4/+ VS R4/CA	ANOVA p-value	Gene	Function	Fold change R4/+ VS R4/CA	ANOVA p-value
impl2	Insulin Signaling	1.88	0.00749	Pepck	Gluconeogenesis	-2.37	0.00476
ilp6	Insulin Signaling	1.98	0.09695	fbp	Gluconeogenesis	-1.6	0.00067
ilp3	Insulin Signaling	-1.81	0.00724	ACC	Fatty acid metabolism	-1.73	0.00299
tobi	Insulin Signaling	1.78	0.00210	Lsd-1	Lipid metabolic processes	-1.96	0.00049
Thor	Insulin Signaling	1.85	0.02917	Lsd-2	Lipid metabolic processes	-1.84	0.00275
Nlaz	Insulin Signaling	2.88	0.00014	Mal-A8	Glycogen metabolic processes	3.23	0.00034
Sug	Insulin Signaling	-1.63	0.00389	Mal-A7	Glycogen metabolic processes	3.64	0.00006
CCHa2	Insulin Signaling	-1.7	0.00662	Mal-A6	Glycogen metabolic processes	2.95	0.00001
AkhR	Carbohydrate homeostasis	-2.17	0.00605	Mal-A5	Glycogen metabolic processes	1.99	0.04195
Tps1	Trehalose biosynthetic process	-2.32	0.00083	Mal-A4	Glycogen metabolic processes	1.8	0.00604
Hex-C	Glycolysis	-3.34	0.00007	Amy-d	Glycogen metabolic processes	4.68	0.00313
Ald	Glycolysis	-1.61	0.00046	Amyrel	Glycogen metabolic processes	1.84	0.01072

Figure 2. Constitutive IMD activation in the larval fat body alters host biological processes.

(A) Gene interaction network of metabolic functions altered in *R4/ImdCA* larvae relative to *R4/+* larvae. Red and blue nodes indicate downregulated and upregulated KEGG terms, respectively. Lines indicate genes shared between nodes, and node size indicates gene number per node. **(B)** Representative signaling pathways altered in *R4/ImdCA* larvae relative to *R4/+* larvae. **(C)** Graphical representation of biological processes dysregulated in *R4/ImdCA* larvae relative to *R4/+* larvae. **(D)** Fold change in the expression of genes involved in insulin signaling, glycolysis, fatty acid metabolism, gluconeogenesis and glycogen metabolism in *R4/ImdCA* larvae relative to *R4/+* larvae.

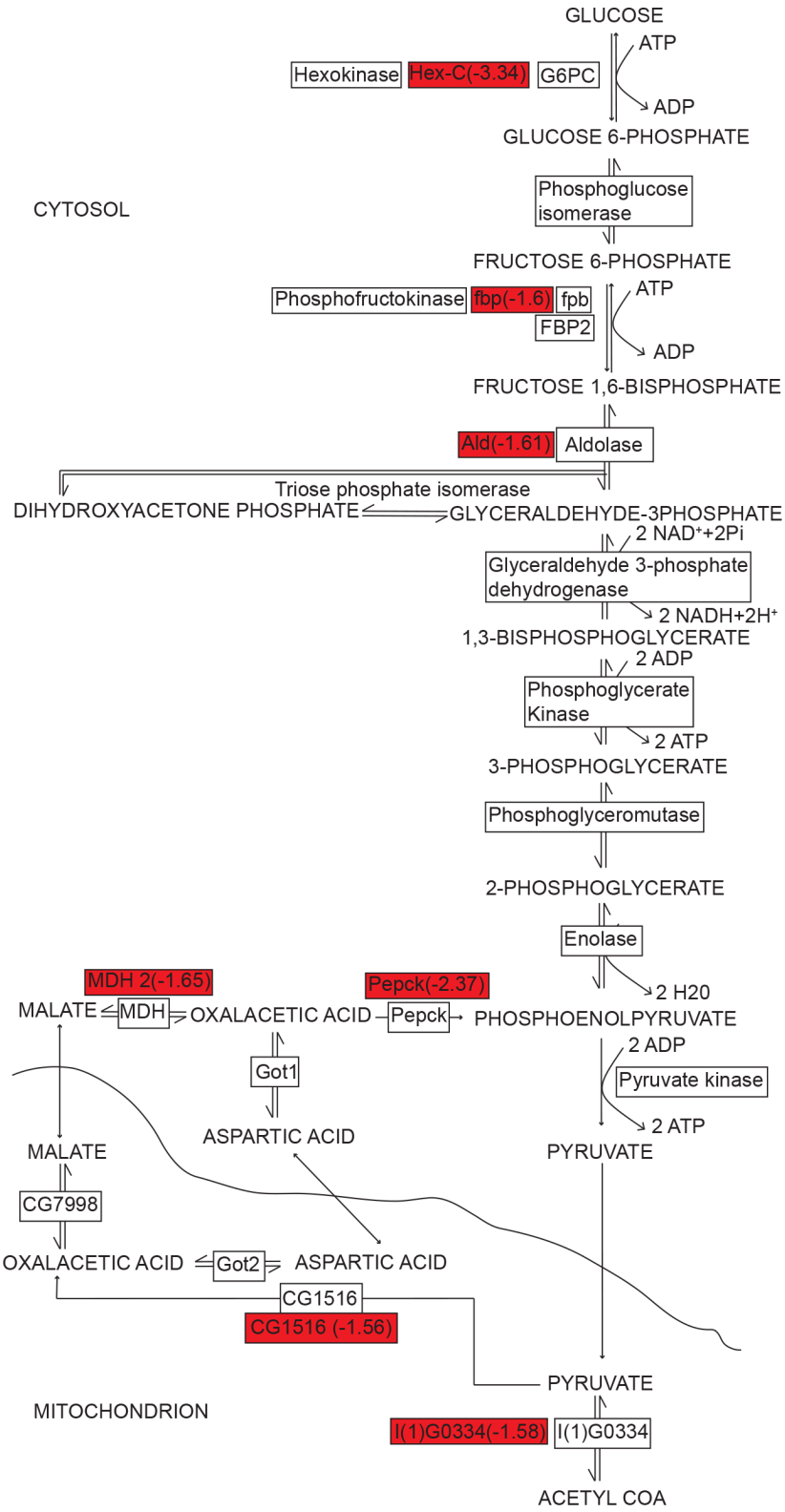

Figure 3. Constitutive IMD activation in the fat body disrupts glycolysis.

Red boxes show downregulated enzymes in *R4/ImdCA* larvae, and numbers indicate degree of downregulation.

We previously characterized the consequences of IMD activation in adult intestinal progenitor cells (Petkau *et al.*, 2017). This allowed us to compare host responses to IMD activation in the fat body, the principle regulator of humoral immunity, to immune activation in the midgut, the first line of defense against intestinal infection. Interestingly, we observed minimal overlap between the two responses (Figure 4 A-C). Only 9.8% of genes affected by IMD activation in the fat body were affected by IMD activation in intestinal progenitors (Figure 4A). These observations suggest broad tissue autonomy in IMD responses. In contrast, 29.8% of genes affected by IMD activation are also affected by loss of the insulin receptor in fat tissue (Musselman *et al.*, 2017) (Figure 4D, E). The overlap between the two gene sets includes genes required for fatty acid beta-oxidation, carbohydrate metabolism, and the TCA cycle. Combined, these results show that activation of IMD in larval fat significantly impacts cellular pathways that regulate metabolism.

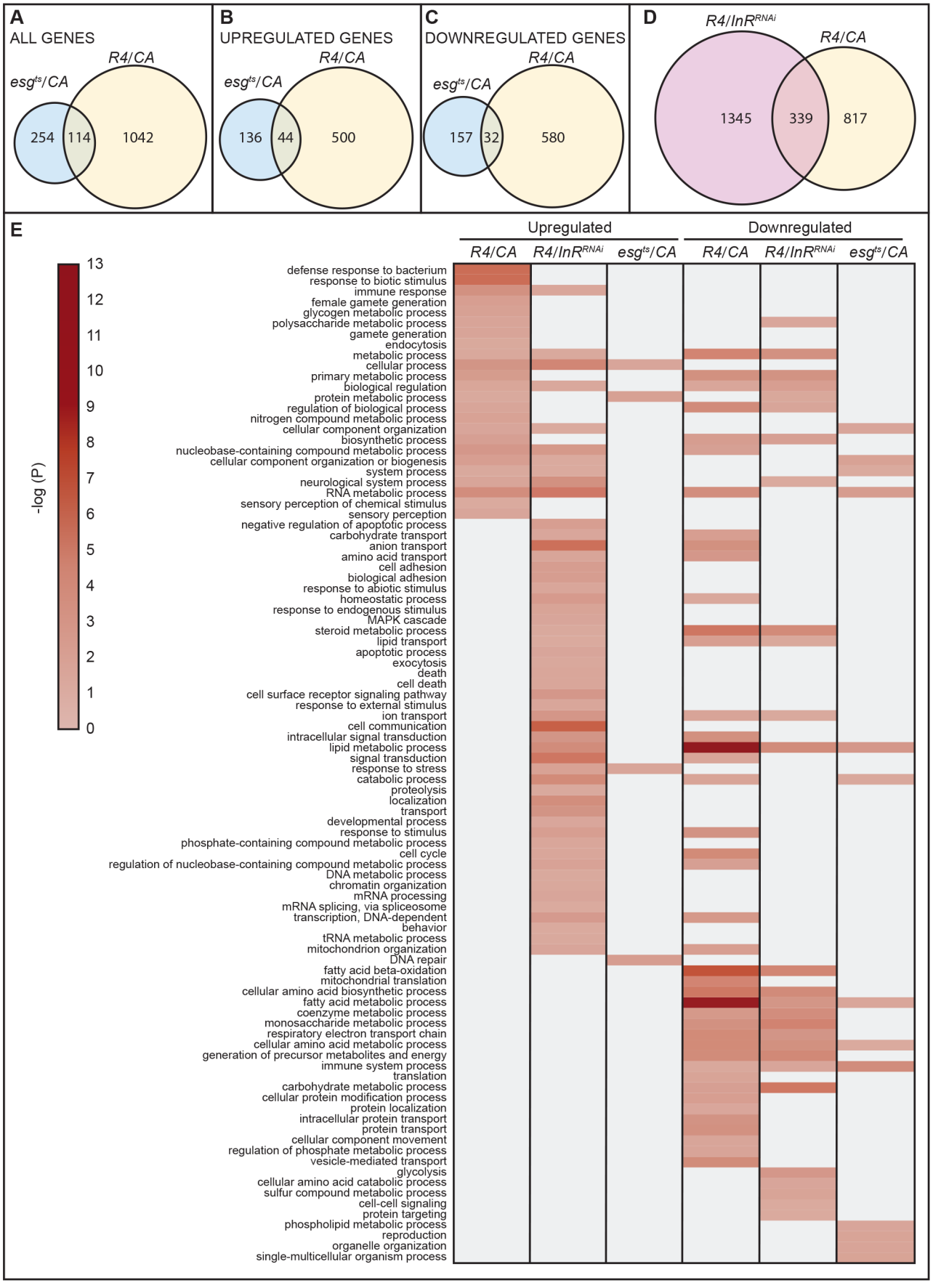

Figure 4. Comparison between constitutive IMD activation in the fat body, intestinal progenitor cells, and larvae with insulin signaling inhibition in the fat body.

(A - C) Overlap between all dysregulated genes in *R4/ImdCA* larvae and *esg^{ts}/ImdCA* intestines. The *esg^{ts}* transgenic line allows inducible transgene expression in intestinal stem cells. (A) upregulated genes (B), and downregulated genes (C). **(D)** Overlap between dysregulated genes in *R4/ImdCA* larvae and *R4/InR^{RNAi}* larvae. **(E)** Heat-map of dysregulated GO terms in *R4/ImdCA* larvae, *esg^{ts}/ImdCA* intestines, and *R4/InR^{RNAi}* larvae.

IMD activation in the fat body disrupts energy reservoirs in the larvae

Our microarray data suggest a possible impact of IMD on the generation, and receipt of signals through the insulin pathway. As insulin stimulates the uptake of circulating carbohydrates, and the storage of energy in the form of glycogen and triacylglycerides (TAG) (Teleman, 2010; Padmanabha and Baker, 2014), we asked what effect IMD activation has on larval energy stores. To answer this question, we first measured total and circulating carbohydrate levels in *R4/imdCA* and *R4/+* larvae. We did not detect obvious effects of IMD on total glucose levels in the larva (Figure 5B). However, we found that activation of IMD resulted in significantly higher levels of circulating trehalose, the primary form of circulating carbohydrate in *Drosophila* (Figure 5A). On average, circulating trelaholse levels were approximately twice as high in *R4/imdCA* larvae as *R4/+* larvae (Figure 5A). We then examined the effects of IMD activation on TAG stores. *Drosophila* larvae store TAG in large lipid droplets in the fat body. The lipid storage droplet 1 (Lsd1) and 2 (Lsd2) proteins are involved in lipid storage and lipolysis control, respectively (Bi *et al.*, 2012), and we found that activation of IMD suppressed the expression of both (Figure 2D). To determine if IMD activation affects TAG stores, we measured total TAG levels, and lipid droplet size in third instar *R4/imdCA* and *R4/+* larvae. We found that activation of IMD decreased total

TAG levels by approximately 50% (Figure 5C), and caused a significant drop in the total volume of lipid stores in the fat body (Figure 5D). Together, these results demonstrate that activation of IMD in the fat body causes hyperglycemia, and a depletion of lipid stores. These data are consistent with an antagonistic impact of IMD on the insulin response pathway.

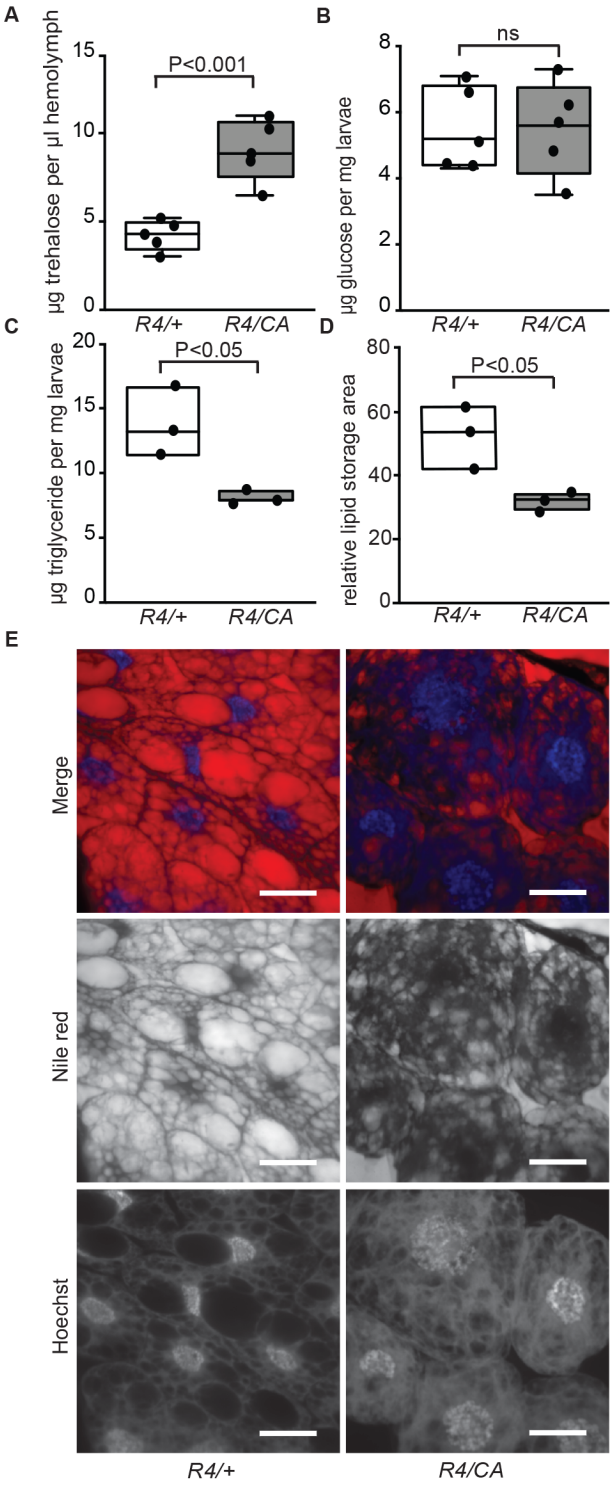

Figure 5. IMD disrupts energy reservoirs in the larvae.

(A-C) Measurement of circulating trehalose (A), total glucose (B) and total triglyceride (C) in *R4/ImdCA* and *R4/+* third instar larvae. **(D)** Quantification of total Nile-red staining area of lipid droplets from third

instar larvae after 6 hours starvation. **(E)** Visualization of lipid droplets in third instar *R4*/*ImdCA* and *R4*/*+* larvae. Fat tissue was stained with Nile-red (lipid droplets) and Hoechst (nuclei). Scale bars, 25 µm. All Statistical significance was determined using a Student's t test.

IMD activation in the fat body delays development and reduces pupal size

As nutrient availability influences larval development (Britton and Edgar, 1998), we determined the effects of IMD activation on larval development. We were specifically interested in the length of time to pupariation, the size of pupae, and the rate of pupal eclosion. Each of these factors is sensitive to metabolite availability and cues from the insulin pathway. In each assay, we noted significant effects of IMD activation on larval development. Specifically, we found that IMD delayed the duration of development from feeding third instar larvae to the P13 stage of pupal development by approximately eighteen hours (Figure 6A); IMD activation led to a roughly 10% drop in pupal volume (Figure 6B); and IMD activation caused a significant reduction in adult eclosion rates compared to *R4*/*+* controls (Figure 6C). These data demonstrate that persistent activation of the IMD pathway significantly disrupts larval development.

The results described to this point are highly consistent with inhibitory effects of IMD on the insulin pathway. Activation of IMD elevated the expression of IIS antagonists, and lowered the expression levels of *dilp3* (Figure 2D). In addition, activation of IMD phenocopies loss of function mutants in the insulin pathway. For example, expression of ImdCA resulted in elevated levels of circulating sugar (Figure 5A), loss of TAG stores (Figure 5C-D), and impaired larval development (Figure 5A-C). These results prompted us to ask if activation of IMD supresses the transduction of signals along the insulin axis. In *Drosophila*, insulin responds to dietary nutrients to promote cellular and organism growth activation of a conserved PI3Kinase/AKT kinase pathway. Nutrients also stimulate growth via activation of a TOR

kinase pathway (S6k) (Grewal, 2009). To determine if IMD affects insulin signaling, we used Western blots to measure the extent of S6k and AKT phosphorylation in *R4/ImdCA and R4/+* larvae in four biological replicates. In each replicate, we noticed a modest reduction in the phosphorylation of S6K, and AKT in *R4/ImdCA* larvae relative to *R4/+* controls (Figure 6D). Combined, these data indicate that activation of IMD in fat tissue suppresses insulin responses in the host.

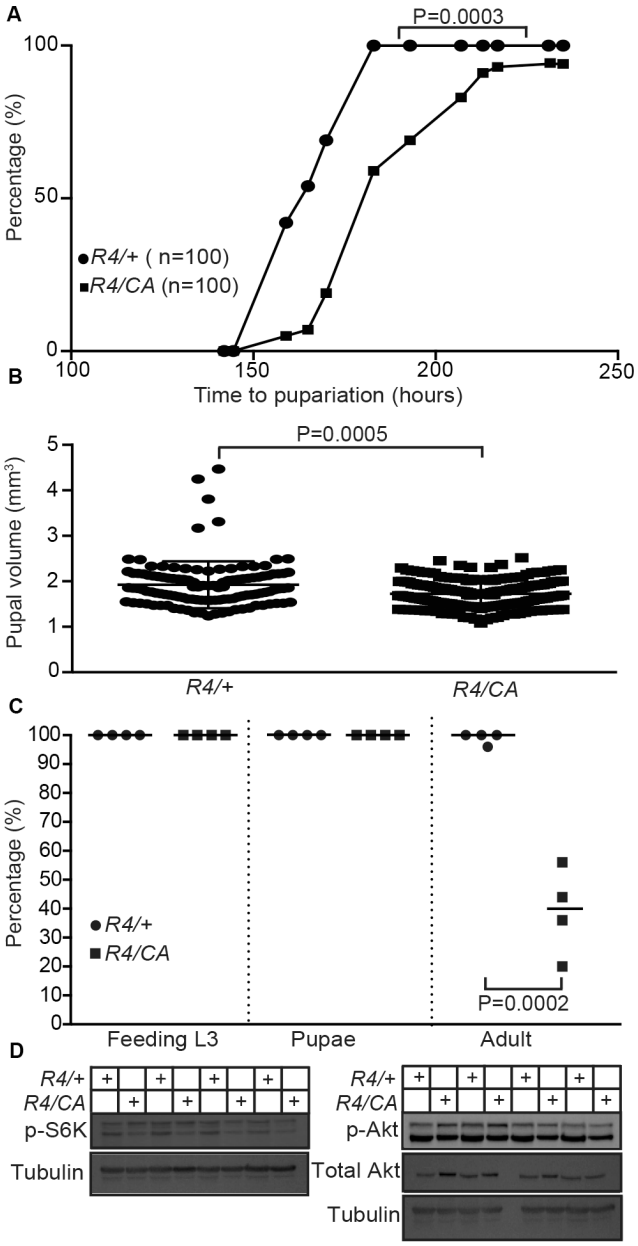

Figure 6. IMD activation impacts larval development.

(A) Pupariation timing of third instar larvae to P13 stage of pupal development. Statistical significance was determined using a KS test. **(B)** Quantification of pupal volume in *R4/ImdCA* and *R4/+ Drosophila*. Statistical significance was determined using a Mann Whitney test. **(C)** 25 feeding third instar larvae of the indicated genotypes were monitored for their development as third instar lavae, pupae, and adults. Results are shown for four independent measurements. **(D)** Immunoblots of whole lysate from third instar larvae.

Reduced insulin activity induces resistance against an enteric pathogen

Previous work showed that TNF suppresses insulin signaling (Hotamisligil, Shargill and Spiegelman, 1993a). Our work shows that IMD, an evolutionary relative of the TNF pathway, also attenuates the transduction of insulin signals in *Drosophila*. This led us to hypothesize that immune-suppression of the insulin response benefits host responses to microbial challenge. To test this hypothesis, we determined the responses of *Drosophila* insulin pathway mutants to lethal challenges with the enteric pathogen *Vibrio cholerae* (*V. cholerae*). For these assays, we initially measured the viability of *R4GAL4/UASimdCA, GAL80^{ts}* (*R4/ImdCA^{ts}*) adults that we challenged with the C6706 strain of *V. cholerae*. Use of the *GAL80^{ts}* construct restricts gene expression to fat tissue of flies incubated at 29°C. We shifted *R4/ImdCA^{ts}* adults to 29°C to activate IMD exclusively in the adult fat body, and measured survival rates after infection. We found that activation of IMD in adult fat attenuated *V. cholerae* lethality (Figure 7), suggesting systemic benefits to immune activation in fat tissue.

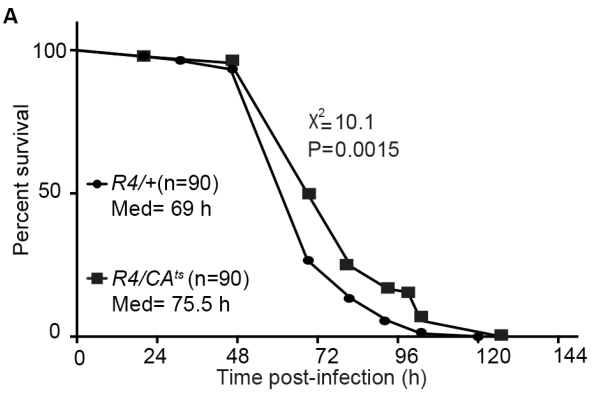

Figure 7. Constitutive IMD activation in the fat body improves survival against infection. Survival curve for oral infection of *R4/+ and R4/ImdCA^{ts}* flies. Statistical significances for survival curve was determined with a Log-rank test. n=number of flies tested. Med=median viability.

We extended this work to determine if insulin pathway mutants phenocopy IMD activation. Here, we found that *ilp2,3,5* mutants survive significantly longer in response to the infection than their wild type counterparts (Figure 8A). Consistent with a beneficial effect of insulin pathway suppression for immune responses to *Vibrio*, we noticed a significant reduction in the intestinal load of *Vibrio cholerae* 24 and 48 hours after infection of *ilp2,3,5* mutants compared to controls (Figure 8C). To further assess if the insulin pathway modifies host survival post infection, we infected *Impl2^{def20}* mutant flies with *V. cholerae. Impl2^{def20}* is an amorphic mutation in the IGFBP7 ortholog Impl2, an antagonist of insulin signaling (Andersen *et al.*, 2000). Loss of Impl2 resulted in reduced survival compared to controls (Figure 8B), and a significantly higher bacterial load post-infection compared to controls (Figure 8D). In short, suppression of insulin activity enhances survival after infection, while elevated insulin signaling diminishes survival rates.

We then asked if insulin modifies survival rates by influencing host resistance or tolerance. Resistance and tolerance are defined as the ability of the host to reduce the pathogen load, and to limit the impacts of the pathogen, respectively (Medzhitov, Schneider and Soares, 2012). To test if mutations

in insulin boost resistance by increased expression of antibacterial effector molecules, we looked at antimicrobial peptide expression in wild type flies, and in *ilp2,3,5* mutants before and after infection. We found that *ilp2,3,5* mutants have a significantly higher level of *drosomycin* prior to infection (Figure 8E). These results match an earlier report that FOXO controls the expression of *drosomycin* in the adult intestine (Becker *et al.*, 2010), and support a role for insulin in controlling resistance to infection. However, these data do not exclude the possibility that insulin influences disease progression by additional mechanisms. For example, in *C. elegans* insulin signaling governs avoidance behavior in response to pathogenic microbes (Lee and Mylonakis, 2017). To determine if insulin has similar effects on *Drosophila*, we measured food consumption in wild-type and *ilp2,3,5* mutants, before and after infection with *Vibrio cholerae*. We found that *ilp2,3,5* mutants consume significantly less food compared to the controls in both cases (Figure 8E). This result is in line with our observation that *ilp2,3,5* mutants have a reduced bacterial load and suggests that inactivation of insulin may diminish the consumption of pathogenic bacteria.

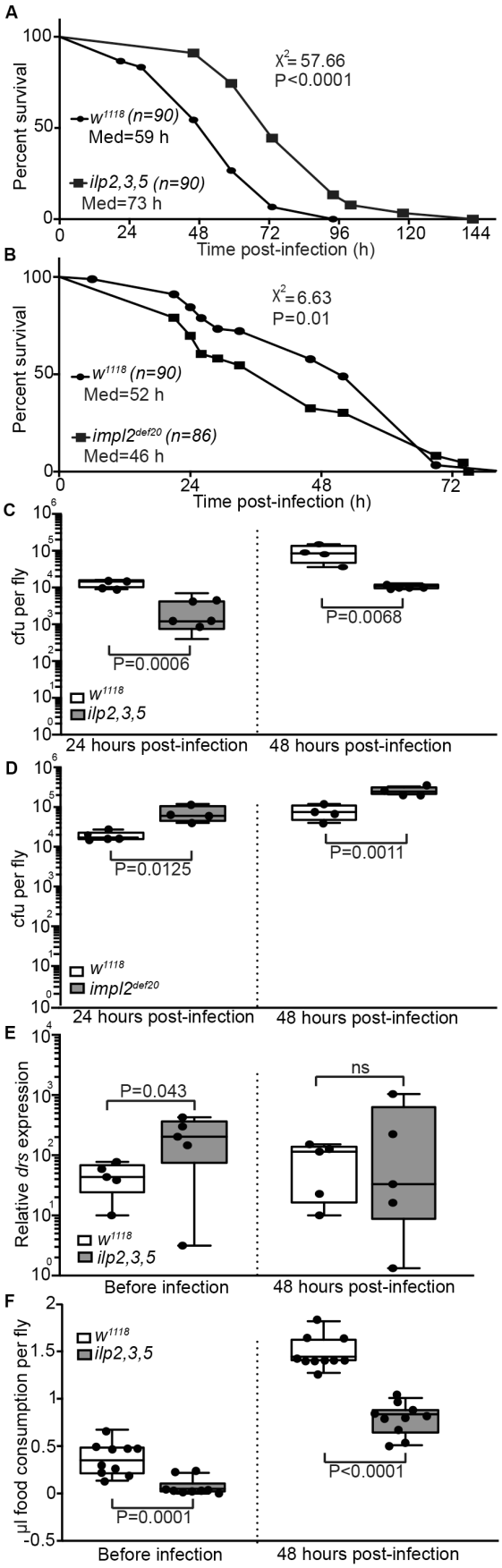

Figure 8. Insulin mutant flies improve immunity against *Vibrio cholerae* infection.

(A-B) Survival curves for w^{1118} and *ilp2,3,5* mutant flies infected with *V. cholerae* (A), or w^{1118} and $impl2^{def20}$ mutant flies infected with *V. cholerae* (B). n=number of flies tested. Med=median viability. Statistical significance was determined using a Log-rank test. **(C-D)** *V. cholerae* colony forming units per w^{1118} and *ilp2,3,5* mutant flies after 24 and 48 hours infection (C), and per w^{1118} and $impl2^{def20}$ mutant flies after 24 and 48 hours infection (D). **(E)** Relative expression of *drosomycin* in guts dissected from w^{1118} and *ilp2,3,5* mutant flies before, and 48 hours after infection with *V. cholerae*. **(F)** Food consumption rates per fly of w^{1118} and *ilp2,3,5* mutant flies before, and 48 hours after infection with *V. cholerae*.

DISCUSSION

Eukaryotic life emerged in an environment dominated by microbes and buffeted by unpredictable periods of nutrient scarcity. In response to these challenges, eukaryotes evolved growth and defense responses that support the complexities of multicellular existence. Both responses act in concert to sustain homeostasis, and disruptions to one pathway often impact the other (Hotamisligil, 2006). This relationship is particularly evident in insects such as *Drosophila* that rely on their fat body to simultaneously coordinate humoral immunity and nutrient utilization. The fat body detects the nutritional and microbial content of the hemolymph and dictates systemic responses designed to maximize host viability. The situation is more complex in higher vertebrates where distinct tissues execute metabolic and immune duties. Nonetheless, the organs in question remain in close communication. For example, obesity results in recruitment of macrophages to adipose tissue (Weisberg *et al.*, 2003; Xu *et al.*, 2003), and induces expression of the TNFα adipokine in adipocytes, with consequences for metabolism and inflammation (Hotamisligil, Shargill and Spiegelman, 1993a). We used *Drosophila* to define the impact of chronic IMD activity exclusively in the fat body. The IMD and TNF signal transduction pathways are closely related, and several recent studies implicated IMD in the regulation of metabolism (Broderick, Buchon and Lemaitre, 2014; Erkosar Combe *et al.*, 2014; Petkau *et al.*, 2017). Our experimental approach allowed us characterize the immune-metabolism axis without requirements for tissue damage. We showed that constitutive IMD activity replicates many phenotypes associated with impaired insulin signaling. Activation of IMD depletes fat reservoirs, causes hyperglycemia, delays development, and causes a reduction in pupal volume. As links between immune activity and insulin appear evolutionarily conserved, we hypothesized that suppression of the insulin pathway improves host survival after infection. Consistent with this hypothesis, we found that insulin pathway mutants have distinct responses to an enteric pathogen.

Our findings that IMD specifically affects insulin activity collaborate reports that the *Drosophila* TNFα homolog, Eiger, regulates production of insulin peptides in the brain (Agrawal *et al.*, 2016), and that the FOXO homolog, Forkhead, regulates intestinal metabolism, and survival after infection in adult *Drosophila* (Bolukbasi *et al.*, 2017). In addition, several studies identified interaction points between immune and insulin responses in the fly. For example, depletion of the insulin receptor from the fat body alters the expression of immune response genes, and alters sensitivity to infection (Musselman *et al.*, 2017). Furthermore, mutations of the IRS homolog *chico* increase survival after infection with *Pseudomonas aeruginosa* and *Enterococcus faecalis* (Libert *et al.*, 2008); challenges with *Mycobacterium marinum* lower AKT phosphorylation, and diminish systemic insulin activity (Dionne *et al.*, 2006); activation of TOR blocks AMP expression (Varma *et al.*, 2014); infection increases expression of the FOXO-responsive transcript 4E-BP ortholog *thor* (Bernal and Kimbrell, 2000); and FOXO regulates the expression of intestinal antimicrobial peptides (Becker *et al.*, 2010). Combined, these findings suggest a direct relationship between bacterial challenges and insulin-sensitive pathways in the fly. This hypothesis is supported by observations that infection with *M. marinum* lowers stores of triglyceride and increases the amount of circulating sugar (Dionne *et al.*, 2006), while challenges with *Listeria monocytogenes* lowers triglyceride and glycogen stores, and inhibits glycolysis (Chambers, Song and Schneider, 2012), and that starvation, or protein restriction increases the expression of antimicrobial peptides (Burger *et al.*, 2007; Lee *et al.*, 2017). An earlier study established that activation of the IMD-responsive NF-κB family member Relish fails to affect insulin signaling in the fly (DiAngelo *et al.*, 2009), suggesting that the IMD-JNK axis is responsible for immune-regulation of insulin signals. In agreement with this hypothesis, several reports link JNK and insulin activity in *Drosophila* (Wang, Bohmann and Jasper, 2005; Karpac *et al.*, 2009).

Connections between insulin and immune activity appear conserved through evolution. In *C. elegans*, mutations in the insulin receptor homolog age-1, the PI3-kinase homolog daf-2, or the FOXO homolog daf-16 impact survival after bacterial infection (Garsin *et al.*, 2003; Kurz and Tan, 2004). Furthermore, protein restriction improves survival against malaria infections in mice (Mejia *et al.*, 2015), while TNFα regulates glucose and lipid levels in vertebrates (Ventre *et al.*, 1997). Experimentally-induced obesity increases the levels of circulating TNFα (Hotamisligil, Shargill and Spiegelman, 1993b), and TNFα makes mice less sensitive to insulin signaling, possibly through the regulation of GLUT4 and IRS-1 (Stephens, Lee and Pilch, 1997). In humans, nutrient excess leads to an inflammatory state characterized by excess TNF production, and increased insulin resistance (Lehrke *et al.*, 2004). Our present work together with these findings indicate that activation of immune responses in a metabolic organ leads to systemic immune-metabolism alterations in the host.

Mechanistically, it is unclear how the insulin pathway modifies immune responses. FOXO regulates antimicrobial peptide expression in the fly, and in human cell culture assays (Becker *et al.*, 2010; Fink *et al.*, 2016). Our data support the hypothesis that a systemic decrease in insulin signaling results in FOXO-induced expression of antimicrobial peptide and improved immunity for the host. However, this immunity might be only induced in intestinal epithelial cells, as previous studies showed that FOXO mutants live longer after a septic infection with *M. marinum* (Dionne *et al.*, 2006). Therefore, unraveling the mechanism of immunity induced by FOXO requires further investigation. We also found that insulin-deficient flies consume fewer pathogens, suggesting microbe avoidance as an additional factor in insulin-dependent regulation of host immunity. We consider it possible that the exact impact of insulin on host responses to microbial challenge depends on the ability of the respective pathogen to navigate altered metabolism in the host. For example, in mice glucose improved survival outcomes in mice challenged with virus, but has the opposite effect in bacterial

infection (Wang *et al.*, 2016). This study outlines an accessible model to characterize the relationship between insulin and IMD/TNF-dependent containment of infectious microbes.

EXPERIMENTAL PROCEDURES

Drosophila methods

Adult flies and larvae were raised on standard corn meal medium (Nutri-Fly Bloomington Formulation https://bdsc.indiana.edu/information/recipes/bloomfood.html, Genesse Scientific). Flies that were used in this study are as follows: w^{1118}, *R4-GAL4, UAS-ImdCA,* $GAL80^{ts}$, $impl2^{def20}$ *and ilp2,3,5*. To measure developmental rates, 25 age-matched feeding third instar larvae were cultured at 25°C and monitored for the formation of wandering third instar larvae, pupae and eclosed adults. For pupariation timing, 25 age-matched third instar larvae were cultured at 25°C and monitored for the length of time required for development to the P13 pupal stage. Developmental and pupariation assays were performed in quadruplicate. For total triglyceride measurement, 10 third instar larvae were weighed and homogenized in TE buffer with 01.% Triton X-100. Triglyceride content was measured in larval homogenate using the serum triglyceride determination kit (Sigma TR0100), according to manufacturer's instructions. Total glucose was measured by homogenizing ten third instar larvae in TE buffer and measuring glucose using the GAGO glucose assy kit (Sigma, GAGO20) according to manufacturer's instructions. For trehalose hemolymph measurements, groups of 15 third instar larvae were dipped in halocarbon oil 700 (Sigma) and the epidermis was punctured to start hemolymph bleeding. Accumulated hemolymph on the oil drop was aspirated using a glass pipette and immediately frozen on dry ice. 1 μl of hemolymph was mixed with 99 μl trehalase buffer (5mM Tris pH 6.6, 137mM NaCl, 2.7mM KCl) and heated at 70°C for 5 minutes to inactivate endogenous Trehalase. The samples were treated with or without Porcine Kidney Trehalase (T8778-1UN, sigma) and incubated at 37°C for 16 hours, then the reaction was started by adding glucose assay reagent (GAGO20, Sigma), incubated at 37°C for 30 minutes, and the reaction was stopped by adding 12 N sulfuric acid. Absorbance were measured at 540 nm. To calculate trehalose levels, we subtracted glucose levels in untreated samples from glucose levels

of samples that were treated with trehalase. CAFE assays were performed as described previously (Diegelmann et al., 2017). Capillaries delivered liquid food (5% sucrose and 5% yeast in deionized water) to the fly. Each chamber contained 3 capillaries with 10 adult flies. Total consumption was calculated after 24 hours. For Nile Red staining, ten third instar larvae were dissected in PBS, and fixed in 4% formaldehyde for 30 minutes. After twice washing with 1X PBS, fat tissues were stained with 1:1000 of a Nile red stock (0.5 mg/ml in acetone) and 1:500 of Hoechst 33258 for 30 minutes. Stained tissue was mounted on slides and visualized using a spinning disk confocal microscope (Quorum WaveFX). Lipid area was quantified with Columbus software (Perkin Elmer). Pupal volume was calculated as previously described (Delanoue et al., 2010). In brief, 24 hr AEL larvae were collected and put into food vials in groups of 50 larvae. Using a paintbrush, 1 day old pupae were picked off the side of the vial. Pupae were imaged using a Zeiss Stereo Discovery V8 microscope using a 14X magnification. Axiovision software was used to measure the length and width of each pupae. Pupal volume was calculated with the assumption that the pupae are cylindrical using the formula: $(4/3\pi)x(length/2)x(diameter/2)^2$.

Bioinformatics

For microarray studies, we used the GeneChip *Drosophila* Genome 2.0 Array (Affymetrix) to measure gene expression in triplicate assays. Total RNA was extracted from third instar larvae using Trizol. We used 100 ng purified RNA to make labeled cRNA using the GeneChip 3' IVT Plus Reagent Kit (Affymetrix). We used Transcriptome Analysis Console (TAC) software (Affymetrix) for preliminary analysis of gene expression data. Array data has been submitted to the NCBI GEO database (accession ID: GSE109470). Transcriptome data from *R4*/*ImdCA* relative to *R4*/*+* larvae was analyzed using GSEA (Subramanian *et al.*, 2005) to identify KEGG pathways that were differentially regulated upon activation of IMD, and visualized with Cytoscape. We used Panther (Mi *et al.*, 2017) to identify biological process that were

affected by IMD activation, and FlyMine (Lyne *et al.*, 2007) to determine tissue enrichment of the respective genes in third instar larvae.

Bacterial Methods

For survival experiments, we streaked the C6706 strain of *Vibrio cholerae* from glycerol stocks onto LB plate and grew them overnight at 37°C. The following day, we grew single colonies in LB medium to an OD_{600} of 0.245, and soaked a sterile cotton plug with 3 ml of the bacterial culture in LB. 6-7 days old virgin female flies were fed on the cotton plug, and death was recorded at the indicated time points. For bacterial load quantification, five flies were first surface sterilized by washing in 20% bleach, distilled water, 70% EtOH, and distilled water., homogenized in LB, and particulates were pelleted, then serial dilutions of each supernatant were plated on LB-agar supplemented with streptomycin (100 mg/ml). To quantify *drosomycin* gene expression, 10 guts per replicate of flies were dissected and RNA was extracted as described in gene expression analysis section.

Molecular Techniques

All qPCR measurements were performed with RNA purified from whole larvae using Trizol, and the delta delta Ct method was used to calculate relative expression values. Gene expressions were normalized to *actin*. Primer sequences are provided in supplemental experimental procedures. For Western blots, Larvae were lysed in lysis buffer (20 mM Tris-HCl (pH 8.0), 137 mM NaCl, 1 mM EDTA, 25 % glycerol, 1% NP-40, 50 mM NaF, 1 mM PMSF, 1 mM DTT, 5 mM Na_3VO_4, Protease Inhibitor cocktail (Roche Cat. No. 04693124001) and Phosphatase inhibitor (Roche Cat. No. 04906845001)), and protein concentrations were measured using the Bio-Rad Dc Protein Assay kit II. For each experiment, equal amounts of protein lysates (usually 15 to 40 μg) were subjected to Western blot analysis. Primary antibodies used were,

anti-alpha-tubulin (alpha-tubulin E7, *Drosophila* Studies Hybridoma Bank), anti- phospho-Drosophila Akt Ser505 (Cell Signaling Technology; 4054), and anti-phospho-S6K Thr398 (Cell Signalling Technology; 9209).

Statistical Analyses

All statistical analyses were performed with GraphPad Prism. qPCR data were analyzed with unpaired Student's t tests. Survival data were analyzed with Log-rank (Mantel- Cox) test. For pupariation timing and pupae counting, KS test and ANOVA were used, respectively. Pupal volumes were compared with a Mann Whitney test.

AUTHOR CONTRIBUTIONS

S.D., R.D. S.G., and E.F. conceived and designed experiments; S.D., M.F., R.D. and S.G. performed the experiments; S.D., M.F., R.D. and E.F. performed data analysis and wrote the paper.

ACKNOWLEDGEMENTS

impl2^{def20} *and ilp2,3,5* flies were provided by Young Kwon and Seung Kim, respectively. The C6706 strain of *Vibrio cholerae* was provided by Stefan Pukatzki. The research was funded by grants from the Canadian Institutes of Health Research to EF (MOP77746) and SG (MOP86622), and from NSERC to SG. MF is supported by an AITF scholarship, and RD by a Clark Smith Brain Tumor Centre Graduate Scholarship. We acknowledge microscopy support from Dr. Stephen Ogg at the University of Alberta. Microarrays were processed at the Alberta Transplant Applied Genomics Center.

Legends for Tables.

Table 1. Description of genes downregulated in *R4/ImdCA* relative *R4/+* larvae are available in R4imdCA_table1.

Table 2. Description of genes upregulated in *R4/ImdCA* relative *R4/+* larvae are available in R4imdCA_table2.

REFERENCES

Agrawal, N. *et al.* (2016) 'The Drosophila TNF Eiger Is an Adipokine that Acts on Insulin-Producing Cells to Mediate Nutrient Response', *Cell Metabolism*, 23(4), pp. 675–684. doi: 10.1016/j.cmet.2016.03.003.

Andersen, A. S. *et al.* (2000) 'A new secreted insect protein belonging to the immunoglobulin superfamily binds insulin and related peptides and inhibits their activities', *Journal of Biological Chemistry*, 275(22), pp. 16948–16953. doi: 10.1074/jbc.M001578200.

Ayres, J. S. and Schneider, D. S. (2012) 'Tolerance of Infections', *Annual Review of Immunology*, 30(1), pp. 271–294. doi: 10.1146/annurev-immunol-020711-075030.

Becker, T. *et al.* (2010) 'FOXO-dependent regulation of innate immune homeostasis', *Nature*, 463(7279), pp. 369–373. doi: 10.1038/nature08698.

Bernal, A. and Kimbrell, D. A. (2000) 'Drosophila Thor participates in host immune defense and connects a translational regulator with innate immunity', *Proceedings of the National Academy of Sciences*, 97(11), pp. 6019–6024. doi: 10.1073/pnas.100391597.

Bi, J. *et al.* (2012) 'Opposite and redundant roles of the two Drosophila perilipins in lipid mobilization', *Journal of Cell Science*, 125(15), pp. 3568–3577. doi: 10.1242/jcs.101329.

Bolukbasi, E. *et al.* (2017) 'Intestinal Fork Head Regulates Nutrient Absorption and Promotes Longevity', *Cell Reports*, 21(3), pp. 641–653. doi: 10.1016/j.celrep.2017.09.042.

Boulan, L., Milán, M. and Léopold, P. (2015) 'The systemic control of growth', *Cold Spring Harbor Perspectives in Biology*, 7(12). doi: 10.1101/cshperspect.a019117.

Britton, J. S. and Edgar, B. a (1998) 'Environmental control of the cell cycle in Drosophila: nutrition activates mitotic and endoreplicative cells by distinct mechanisms.', *Development (Cambridge, England)*, 125(11), pp. 2149–2158. Available at:

http://dev.biologists.org/content/develop/125/11/2149.full.pdf.

Broderick, N. A., Buchon, N. and Lemaitre, B. (2014) 'Microbiota-induced changes in Drosophila melanogaster host gene expression and gut morphology', *mBio*, 5(3). doi: 10.1128/mBio.01117-14.

Buchon, N., Silverman, N. and Cherry, S. (2014) 'Immunity in Drosophila melanogaster-from microbial recognition to whole-organism physiology', *Nature Reviews Immunology*, pp. 796–810. doi: 10.1038/nri3763.

Burger, J. M. S. *et al.* (2007) 'The functional costs and benefits of dietary restriction in Drosophila', *Aging Cell*, 6(1), pp. 63–71. doi: 10.1111/j.1474-9726.2006.00261.x.

Chambers, M. C., Song, K. H. and Schneider, D. S. (2012) 'Listeria monocytogenes Infection Causes Metabolic Shifts in Drosophila melanogaster', *PLoS ONE*, 7(12). doi: 10.1371/journal.pone.0050679.

Clark, R. I. *et al.* (2013) 'XMEF2 is an in vivo immune-metabolic switch', *Cell*, 155(2). doi: 10.1016/j.cell.2013.09.007.

DiAngelo, J. R. *et al.* (2009) 'The immune response attenuates growth and nutrient storage in Drosophila by reducing insulin signaling', *Proceedings of the National Academy of Sciences*, 106(49), pp. 20853–20858. doi: 10.1073/pnas.0906749106.

Dionne, M. S. *et al.* (2006) 'Akt and foxo Dysregulation Contribute to Infection-Induced Wasting in Drosophila', *Current Biology*, 16(20), pp. 1977–1985. doi: 10.1016/j.cub.2006.08.052.

Eisenreich, W. *et al.* (2013) 'Metabolic host responses to infection by intracellular bacterial pathogens', *Frontiers in Cellular and Infection Microbiology*, 3. doi: 10.3389/fcimb.2013.00024.

Erkosar Combe, B. *et al.* (2014) 'Drosophila microbiota modulates host metabolic gene expression via IMD/NF-κB signaling', *PloS one*, 9(4), p. e94729. doi: 10.1371/journal.pone.0094729.

Fink, C. *et al.* (2016) 'Intestinal FoxO signaling is required to survive oral infection in Drosophila', *Mucosal Immunology*, 9(4), pp. 927–936. doi: 10.1038/mi.2015.112.

Garsin, D. A. *et al.* (2003) 'Long-lived C. elegans daf-2 Mutants are resistant to bacterial pathogens', *Science*, 300(5627), p. 1921. doi: 10.1126/science.1080147.

Gems, D. and Partridge, L. (2013) 'Genetics of Longevity in Model Organisms: Debates and Paradigm Shifts', *Annual Review of Physiology*, 75(1), pp. 621–644. doi: 10.1146/annurev-physiol-030212-183712.

Grewal, S. S. (2009) 'Insulin/TOR signaling in growth and homeostasis: A view from the fly world', *International Journal of Biochemistry and Cell Biology*, pp. 1006–1010. doi: 10.1016/j.biocel.2008.10.010.

Hotamisligil, G. S. (2006) 'Inflammation and metabolic disorders', *Nature*, pp. 860–867. doi: 10.1038/nature05485.

Hotamisligil, G. S., Shargill, N. S. and Spiegelman, B. M. (1993a) 'Adipose expression of tumor necrosis factor-alpha: direct role in obesity-linked insulin resistance', *Science*, 259(5091), pp. 87–91. doi: 10.1126/science.7678183.

Hotamisligil, G. S., Shargill, N. S. and Spiegelman, B. M. (1993b) 'Adipose expression of tumor necrosis factor-alpha: direct role in obesity-linked insulin resistance.', *Science (New York, N.Y.)*, 259(5091), pp. 87–91. doi: 10.1126/science.7678183.

Kannan, K. and Fridell, Y.-W. C. (2013) 'Functional implications of Drosophila insulin-like peptides in metabolism, aging, and dietary restriction', *Frontiers in Physiology*, 4. doi: 10.3389/fphys.2013.00288.

Karpac, J. *et al.* (2009) 'JNK signaling in insulin-producing cells is required for adaptive responses to stress in Drosophila', *Aging Cell*, 8(3), pp. 288–295. doi: 10.1111/j.1474-9726.2009.00476.x.

Kim, J. K. *et al.* (2001) 'Prevention of fat-induced insulin resistance by salicylate', *Journal of Clinical Investigation*, 108(3), pp. 437–446. doi: 10.1172/JCI200111559.

Kurz, C. L. and Tan, M. W. (2004) 'Regulation of aging and innate immunity in C. elegans', *Aging Cell*,

pp. 185–193. doi: 10.1111/j.1474-9728.2004.00108.x.

Lee, J. (2013) 'Adipose tissue macrophages in the development of obesity-induced inflammation, insulin resistance and type 2 Diabetes', *Archives of Pharmacal Research*, pp. 208–222. doi: 10.1007/s12272-013-0023-8.

Lee, J. E. *et al.* (2017) 'Acute Dietary Restriction Acts via TOR, PP2A, and Myc Signaling to Boost Innate Immunity in Drosophila', *Cell Reports*, 20(2), pp. 479–490. doi: 10.1016/j.celrep.2017.06.052.

Lee, K. and Mylonakis, E. (2017) 'An Intestine-Derived Neuropeptide Controls Avoidance Behavior in Caenorhabditis elegans', *Cell Reports*, 20(10), pp. 2501–2512. doi: 10.1016/j.celrep.2017.08.053.

Lehrke, M. *et al.* (2004) 'An inflammatory cascade leading to hyperresistinemia in humans', *PLoS Medicine*, 1, pp. 161–168. doi: 10.1371/journal.pmed.0010045.

Libert, S. *et al.* (2008) 'Realized immune response is enhanced in long-lived puc and chico mutants but is unaffected by dietary restriction', *Molecular Immunology*, 45(3), pp. 810–817. doi: 10.1016/j.molimm.2007.06.353.

Lyne, R. *et al.* (2007) 'FlyMine: An integrated database for Drosophila and Anopheles genomics', *Genome Biology*, 8(7). doi: 10.1186/gb-2007-8-7-r129.

Medzhitov, R., Schneider, D. S. and Soares, M. P. (2012) 'Disease tolerance as a defense strategy', *Science*, pp. 936–941. doi: 10.1126/science.1214935.

Mejia, P. *et al.* (2015) 'Dietary restriction protects against experimental cerebral malaria via leptin modulation and T-cell mTORC1 suppression', *Nature Communications*, 6. doi: 10.1038/ncomms7050.

Mi, H. *et al.* (2017) 'PANTHER version 11: Expanded annotation data from Gene Ontology and Reactome pathways, and data analysis tool enhancements', *Nucleic Acids Research*, 45(D1), pp. D183–D189. doi: 10.1093/nar/gkw1138.

Murphy, C. T. and Hu, P. J. (2013) 'Insulin/insulin-like growth factor signaling in C. elegans.',

WormBook : the online review of C. elegans biology, (Figure 1), pp. 1–43. doi: 10.1895/wormbook.1.164.1.

Musselman, L. P. *et al.* (2017) 'The relationship between immunity and metabolism in *Drosophila* diet-induced insulin resistance', *Molecular and Cellular Biology*, p. MCB.00259-17. doi: 10.1128/MCB.00259-17.

Myllymaki, H., Valanne, S. and Ramet, M. (2014) 'The Drosophila Imd Signaling Pathway', *The Journal of Immunology*, 192(8), pp. 3455–3462. doi: 10.4049/jimmunol.1303309.

O'Neill, L. A. J., Kishton, R. J. and Rathmell, J. (2016) 'A guide to immunometabolism for immunologists', *Nature Reviews Immunology*, pp. 553–565. doi: 10.1038/nri.2016.70.

Padmanabha, D. and Baker, K. D. (2014) 'Drosophila gains traction as a repurposed tool to investigate metabolism', *Trends in Endocrinology and Metabolism*, pp. 518–527. doi: 10.1016/j.tem.2014.03.011.

Petkau, K. *et al.* (2017) 'Constitutive Immune Activity Promotes Tumorigenesis in Drosophila Intestinal Progenitor Cells', *Cell Reports*, 20(8), pp. 1784–1793. doi: 10.1016/j.celrep.2017.07.078.

Le Roith, D. *et al.* (1980) 'Evolutionary origins of vertebrate hormones: substances similar to mammalian insulins are native to unicellular eukaryotes.', *Proceedings of the National Academy of Sciences of the United States of America*, 77(10), pp. 6184–8. doi: 10.1073/pnas.77.10.6184.

Stephens, J. M., Lee, J. and Pilch, P. F. (1997) 'Tumor necrosis factor-α-induced insulin resistance in 3T3-L1 adipocytes is accompanied by a loss of insulin receptor substrate-1 and GLUT4 expression without a loss of insulin receptor-mediated signal transduction', *Journal of Biological Chemistry*, 272(2), pp. 971–976. doi: 10.1074/jbc.272.2.971.

Subramanian, A. *et al.* (2005) 'Gene set enrichment analysis: A knowledge-based approach for interpreting genome-wide expression profiles', *Proceedings of the National Academy of Sciences*, 102(43), pp. 15545–15550. doi: 10.1073/pnas.0506580102.

Teleman, A. a (2010) 'Molecular mechanisms of metabolic regulation by insulin in Drosophila.', *The Biochemical journal*, 425(1), pp. 13–26. doi: 10.1042/BJ20091181.

Uysal, K. T. *et al.* (1997) 'Protection from obesity-induced insulin resistance in mice lacking TNF-alpha function.', *Nature*, 389(6651), pp. 610–4. doi: 10.1038/39335.

Uysal, K. T., Wiesbrock, S. M. and Hotamisligil, G. S. (1998) 'Functional analysis of tumor necrosis factor (TNF) receptors in TNF-alpha-mediated insulin resistance in genetic obesity.', *Endocrinology*, 139(12), pp. 4832–4838. doi: 10.1210/endo.139.12.6337.

Valanne, S., Wang, J.-H. and Ramet, M. (2011) 'The Drosophila Toll Signaling Pathway', *The Journal of Immunology*, 186(2), pp. 649–656. doi: 10.4049/jimmunol.1002302.

Varma, D. *et al.* (2014) 'Forkhead, a new cross regulator of metabolism and innate immunity downstream of TOR in Drosophila', *Journal of Insect Physiology*, 69(C), pp. 80–88. doi: 10.1016/j.jinsphys.2014.04.006.

Ventre, J. *et al.* (1997) 'Targeted disruption of the tumor necrosis factor-alpha gene: metabolic consequences in obese and nonobese mice.', *Diabetes*, 46(9), pp. 1526–1531. doi: 10.2337/diabetes.46.9.1526.

Wang, A. *et al.* (2016) 'Opposing Effects of Fasting Metabolism on Tissue Tolerance in Bacterial and Viral Inflammation', *Cell*, 166(6), p. 1512–1525.e12. doi: 10.1016/j.cell.2016.07.026.

Wang, M. C., Bohmann, D. and Jasper, H. (2005) 'JNK extends life span and limits growth by antagonizing cellular and organism-wide responses to insulin signaling', *Cell*, 121(1), pp. 115–125. doi: 10.1016/j.cell.2005.02.030.

Weisberg, S. P. *et al.* (2003) 'Obesity is associated with macrophage accumulation in adipose tissue', *Journal of Clinical Investigation*, 112(12), pp. 1796–1808. doi: 10.1172/JCI200319246.

Wellen, K. E. and Hotamisligil, G. S. (2005) 'Inflammation, stress, and diabetes', *Journal of Clinical*

Investigation, pp. 1111–1119. doi: 10.1172/JCI200525102.

Xu, H. *et al.* (2003) 'Chronic inflammation in fat plays a crucial role in the development of obesity-related insulin resistance.', *The Journal of clinical investigation*, 112(12), pp. 1821–30. doi: 10.1172/JCI19451.

Yuan, M. *et al.* (2001) 'Reversal of obesity- and diet-induced insulin resistance with salicylates or targeted disruption of Ikkβ', *Science*, 293(5535), pp. 1673–1677. doi: 10.1126/science.1061620.